PHYSICAL REVIEW B VOLUME 25, NUMBER 2 15 JANUARY 1982

Pressure dependence of Raman phonons of Ge and 3C-SiC

Diego Olego and Manuel Cardona
Max-Planck-Institut für Festkörperforschung, Heisenbergstrasse 1, 7000 Stuttgart 80, Federal Republic of Germany
(Received 10 September 1981)

The pressure dependence of several Raman lines of Ge and 3C-SiC has been studied up to 11 GPa with a gasketed diamond anvil cell. A nonlinear dependence of the TO(Γ) frequencies on pressure and a softening of the TA(X) modes of Ge have been observed. The Grüneisen parameters of several optical and acoustical phonons of 3C-SiC corresponding to critical points at the edges of the zone have been determined. The linewidths of the long-wavelength optical phonons of 3C-SiC increase for pressures above 10 GPa. This observation is interpreted in terms of an increase in the decay rates of the Γ optical phonons into two acoustical modes.

I. INTRODUCTION

The pressure dependence of the phonon spectra of semiconducting materials has received considerable attention in recent years. The development of the diamond anvil cell and the ruby flourescence manometer,[1] together with inelastic light scattering techniques,[2] has made such investigations possible. First- and second-order Raman spectra have been reported at very high pressures, in some cases up to the structural phase transition, for materials with diamond,[2,3] zinc-blende,[2,4–6] and chalcopyrite structures.[7] (Most of these investigations have been aimed at determining the mode-Grüneisen parameter, from which an understanding of the lattice-dynamical properties, especially anharmonicity, can be obtained.)

The first-order Raman spectra are due to scattering by long-wavelength optical phonons, and in polar semiconductors with different atoms in the unit cell a study of the LO- (longitudinal optical) TO (transverse optical) splitting under pressure yields the dependence of their ionicity on volume.[4,5,8] The second-order Raman spectra arise from scattering by two phonons with opposite wave vectors, predominantly near the Brillouin-zone boundaries. Of particular interest is the determination of the *negative* Grüneisen parameters of the transverse acoustical TA(X) phonons. They correspond to an unusual softening of these low-energy modes upon compression. It has been suggested that a linear relationship exists between the negative Grüneisen parameters of the TA modes and the pressures at which the structural phase transitions (mostly from zinc-blende to an NaCl phase) take place.[6] However, exceptions to the proposed relationship have been found (see Fig. 5 of Ref. 7 which summarizes the results for all the material studied), and hence any new data about the pressure dependence of the low-energy phonon modes of other covalent semiconductors can help to clarify this point. Microscopic theoretical calculations of the volume dependence of the phonon energies in Si and Ge account for the experimental results and particularly for the softening of the TA(X) modes.[9,10]

The small sample volumes available with the diamond cell together with the small band gap of Ge have prevented Raman scattering investigations at very high pressures (diamond anvil cell) for this material because of the very weak scattering efficiencies obtained. The only pressure data reported for Ge correspond to the pressure dependence of the TO(Γ) phonon for pressures below 1 GPa obtained with conventional pressure cells.[11] Some information about the hydrostatic pressure coefficient of the optical phonon has also been inferred from Raman scattering measurements under uniaxial stress.[12] The largest hydrostatic components of these uniaxial stresses were approximately 0.3 GPa. We have succeeded in obtaining Raman signals from Ge when placed in a diamond anvil cell. Thus we have measured the pressure dependence of the TO(Γ) phonons for pressures up to the phase transition (~11 GPa). With increasing pressures above 7 GPa Ge became almost transparent to the near-infrared lines of the Kr^+-ion laser.[13] Under these resonant conditions we were also able to ob-

serve second-order Raman scattering by two TA(X) phonons. We have therefore determined the Grüneisen parameter of these modes. It turns out to be negative and fits into the systematics of the covalent bonded semiconductors.

We have already reported the dependence on pressure of the long-wavelength optical phonons (first-order Raman scattering) and of the related properties, namely the Born transverse effective charge.[8] It was shown that the covalency of 3C-SiC diminishes upon lattice compression. To our knowledge the second-order Raman spectra of 3C-SiC or other polytypes have not been investigated previously. By using the pressure coefficients measured for the observed features, together with the phonon dispersion curves of SiC as determined with the folded zones scheme,[14] it is possible to establish from which phonon combination the second-order features arise. The mode-Grüneisen parameters of different phonons at the zone edge have been determined. These results are presented and discussed in this paper.

II. EXPERIMENTAL DETAILS

The Ge samples were prepared by lapping and polishing a piece of p-type single crystal ($N_A \simeq 4\times 10^{14}$ cm^{-3}) down to a thickness of 30 μm. The 3C-SiC samples were cut from single crystals grown at Westinghouse Research Laboratories and kindly given to us by Dr. W. J. Choyke. For the high-pressure measurements the samples were broken into small pieces and one of them, suitable to fit into the 2000-μm hole of the pressure cell gasket, was chosen under the microscope.

A gasketed diamond anvil cell, such as the one described by Syassen and Holzapfel,[15] was employed for the Raman measurements. A 4:1 methanol-ethanol mixture served as the pressure medium, and the fluorescence of a small ruby chip placed near the sample was used for pressure calibration.[1]

The backscattering geometry was adopted to perform the experiment.[2] The Raman spectra of Ge were excited with the 6471-Å (1.92 eV) line of a Kr^+-ion laser and those of 3C-SiC by using the 5145-Å (2.41 eV) line of an Ar^+-ion laser. The scattered light was collected with an f 1:1 focusing lens into the entrance slit of a Spex 1402 double monochromator, equipped with holographic gratings. The detection was made with a cooled RCA 31034 photomultiplier in the photon counting mode. All measurements were carried out at room temperature.

III. RESULTS AND DISCUSSION

A. Ge

Typical first-order Raman spectra of Ge for different values of the pressure are shown in Fig. 1. With increasing pressure the first-order TO(Γ) phonon lines shift to higher energies. Within the experimental uncertainties no change in the TO(Γ) line shapes was observed. For pressures above 11 GPa the Ge samples underwent a structural phase transition and the Raman signal was lost. The measured peak positions of the TO(Γ) Raman lines either as a function of pressure (top horizontal scale) or of the relative lattice compression $-\Delta a/a_0$ (bottom horizontal scale) are displayed in Fig. 2. The Murnaghan equation of state was used to relate the lattice constant a under a pressure p (Refs. 4 and 5):

$$\frac{a}{a_0}=\left[\frac{B_0'}{B_0}p+1\right]^{-1/3B_0'} . \tag{1}$$

In Eq. (1) $B_0=74.37$ GPa is the bulk modulus of Ge and $B_0'=4.76$ is its pressure derivative.[16]

The data of Fig. 2 are plotted against a scale linear in the relative lattice compression $-\Delta a/a_0$. With this choice the measured TO(Γ) phonon energies fall on a straight line which is described with the following least-squares fit:

$$\omega_{\mathrm{TO}(\Gamma)}=(300.1\pm 0.5)+(1027\pm 10)\left[-\frac{\Delta a}{a_0}\right] , \tag{2}$$

with $\omega_{\mathrm{TO}(\Gamma)}$ given in cm^{-1}. When plotted against a linear pressure scale, the $\omega_{\mathrm{TO}(\Gamma)}$ energies show a sublinear dependence with increasing pressure.

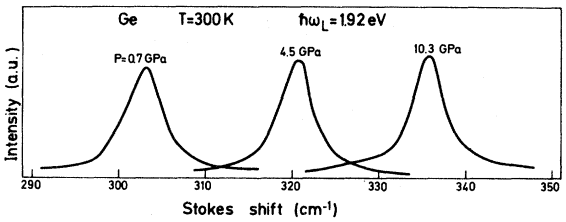

FIG. 1. First-order Raman spectra of Ge recorded for different values of the pressure at room temperature.

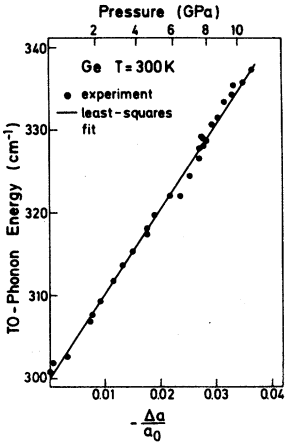

FIG. 2. Measured peak positions of the TO(Γ) phonon Raman lines as a function of lattice compression (linear bottom scale) and of pressure (top horizontal scale). The solid line is a fit to the experimental points with Eq. (2).

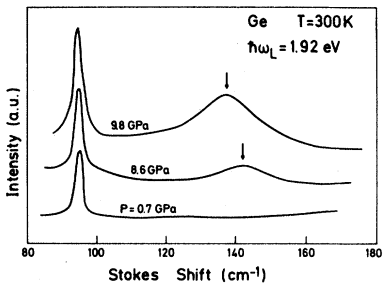

FIG. 3. Second-order Raman spectra of Ge for Stokes shifts near the 2TA(X) phonon energy recorded for different pressures. The line on the left side peaking at around 97 cm^{-1} is a plasma emission line from the laser tube. It can be used as a reference, from which shifts of the other lines are determined. At very high pressures a Raman line develops at around 140 cm^{-1}. With increasing pressure this new line shifts even to lower wave numbers. It has been characterized as arising from scattering by two transverse acoustical modes with wave vectors near X. The fact that this line is only observed for pressures near the phase transitions is due to a resonant enhancement of the scattering efficiency, because above 8 GPa the energy of the direct absorption edge of Ge is comparable with the energy of the incoming laser photons.

The pressure dependence can be represented by

$$\omega_{\mathrm{TO}(\Gamma)} = (300.6\pm0.5)+(3.85\pm0.05)p - (3.9\pm0.6)\times10^{-2}p^2 , \quad (3)$$

with p in GPa and $\omega_{\mathrm{TO}(\Gamma)}$ in cm^{-1}. Quadratic terms in the pressure dependence of phonon energies and of electronic band edges arise in part from the nonlinear relationship between Δa and p given by Eq. (1).[4,13]

From the linear coefficient of Eq. (2) the mode-Grüneisen parameter $\gamma_i = -\partial \ln \omega_i / \partial \ln V$ can be determined. We obtain for the long-wavelength optical phonons of Ge a value of $\gamma_{\mathrm{TO}(\Gamma)} = 1.14\pm0.01$.

Figure 3 displays the low-energy Stokes-Raman spectra of Ge for different pressures. The sharp line which peaks at around 97 cm^{-1} corresponds to a plasma emission line from the laser and can be used for calibration purposes. For pressures near the phase transition a new Raman peak develops around 140 cm^{-1}. This line, which is not present in the spectra at low pressures, shifts to lower energies with increasing pressure as shown in Fig. 3 for 8.6 and 9.8 GPa. This behavior suggests that the new Raman line corresponds to scattering by transverse acoustic modes with wave vectors near X. The fact that this second-order Raman peak is observed only at very high pressures is due to a resonant process: For pressures around 9 GPa the direct band edge of Ge opens to approximately 1.9 eV,[13] an energy very close to that of the incoming laser photons. Consequently, the measurements at very high pressures have been performed under extreme resonant conditions. We attempted to measure the whole second-order Raman spectrum of Ge favored by the resonant enhancement of the scattering efficiency. However, for Stokes shifts larger than 400 cm^{-1} some unidentified features either from the ruby chip or from the methanol-ethanol fluid obscured the Ge Raman signal. Hence we were not able to obtain a clear characterization of the Raman lines and their pressure dependence as in the case of the spectra displayed in Fig. 3.

The measured positions of the Raman peaks shown in Fig. 3 are plotted in Fig. 4 against a scale linear in the relative lattice compression. The value of the 2TA(X) phonon energy for $\Delta a = 0$ (represented by a triangle in the figure) was taken from Ref. 17, in which a study of the second-order Raman spectra of Ge at normal pressure is reported. The solid line through the experimental points is a least-squares fit given by

$$\omega_{2\mathrm{TA}(X)} = (163.1\pm0.5) - (749\pm20)\left[-\frac{\Delta a}{a_0}\right] , \quad (4)$$

with $\omega_{2\mathrm{TA}(X)}$ in cm^{-1}. When plotted against a linear pressure scale the 2TA(X) peak positions can

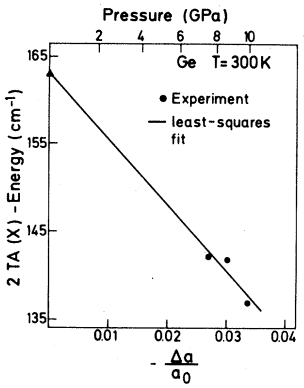

FIG. 4. Measured peak position of the 2TA(X) Raman lines as a function of the relative lattice compression (linear bottom scale) and pressure (upper scale). The data for $\Delta a = 0$ were taken from Ref. 17 and are represented by the triangle. The solid line is a linear fit with Eq. (4).

be described by

$$\omega_{2\mathrm{TA}(X)} = (163 \pm 0.5) - (2.61 \pm 0.05)p \ , \qquad (5)$$

with $\omega_{2\mathrm{TA}(X)}$ in cm^{-1} and p in GPa. The mode-Grüneisen parameter of the TA(X) phonons is determined to be from Eq. (4): $\gamma_{\mathrm{TA}(X)} = -(1.53 \pm 0.05)$. Table I summarizes the pressure coefficients and mode-Grüneisen parameters obtained for the TO(Γ) and TA(X) phonons of Ge. Other available experimental data are also tabulated. The agreement between the low-pressure results and those reported in this paper is good, particularly for the Grüneisen parameters.

Recently, a microscopic theoretical calculation has been performed for the volume dependence of the phonon frequencies and mode-Grüneisen parameters of Ge and Si.[9,10] The results of the theory for Ge are also tabulated in Table I and compared with the experiment. This theory accounts rather well for the experimental results.

We investigate now for Ge the relationship between $\gamma_{\mathrm{TA}(X)}$ and the transition pressure which was proposed in Ref. 6 for the covalent semiconductors. In the case of Ge we have plotted $\gamma_{\mathrm{TA}(X)} = -1.53$ against the transition pressure of 11 GPa in Fig. 5, together with similar data for other materials obtained from the plots of Refs. 4 and 7. Germanium seems to fulfill the empirical linear relationship proposed for $\gamma_{\mathrm{TA}(X)}$ as a function of the transition pressure.[6] On the other hand, the relative softening of the TA(X) modes just before the phase transition takes place is for Ge the lowest as compared with other zinc-blende-type semiconductors. The TA(X) frequency of the phase transition is 0.82 of the zero-pressure value. For other materials a value of 0.7 was often found (see Table VI in Ref. 7).

B. 3C-SiC

In this section we present and discuss the pressure dependence of the features observed in the second-order Raman spectra of 3C-SiC. Figure 6 displays typical spectra recorded at different pressures. We will consider the dependence on pressure of the Raman peaks labeled from a to g. These peaks were always present for different loadings of the diamond cell and were also observed with the sample outside of the cell. In Fig. 6 three very strong Raman lines are also displayed. Two of them labeled TO(Γ) and LO(Γ) are the first-order Raman lines of 3C-SiC. The pressure dependence of these lines has been the subject of a previous publication.[8] The third strong line is the first-order Raman line of the diamond anvil.[18] This line remains almost at the same position independently of pressure. The intensities of the lines $a-g$ decreased with increasing pressure. We

TABLE I. Experimental and theoretical pressure coefficients and mode-Grüneisen parameters of the TO(Γ) and TA(X) phonons of Ge.

Phonon mode	$\frac{d\omega}{dp}$ ($\mathrm{cm}^{-1}\,\mathrm{GPa}^{-1}$) Experiment	Theory	Grüneisen parameter Experiment	Theory
TO(Γ)	3.85 ± 0.05[a]	4.7 ± 0.1[c]	1.14 ± 0.01[a]	1.1 ± 0.1[c]
	4.6 ± 0.1[b]		1.12 ± 0.02[b]	
TA(X)	-1.31 ± 0.02[a]	-1.7 ± 0.4[c]	-1.53 ± 0.05[a]	-1.2 ± 0.1[c]

[a]This work.
[b]Reference 11 (pressures up to 1 GPa).
[c]Reference 10.

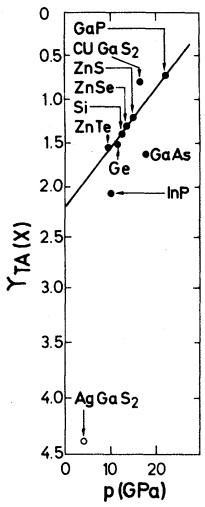

FIG. 5. Grüneisen parameter $\gamma_{TA(X)}$ for a number of covalent-type semiconductors plotted as a function of the pressures at which the structural phase transition take place. Our results for Ge seem to fulfill the linear relationship proposed in Ref. 6.

could follow their pressure dependence up to 11 GPa. The first-order TO(Γ) and LO(Γ) lines have been measured up to 22.5 GPa.[8] The decrease of the scattering efficiency of some of the second-order lines is probably related to the pressure dependence of the indirect electronic gap $(X_1^c - \Gamma_{15}^v)$ of 3C-SiC. This gap is the smallest one for 3C-SiC and has at normal pressure for $T = 300$ K a value of approximately 2.40 eV,[19] which is very close to the energy of the incoming laser photons ($\hbar\omega_L = 2.41$ eV). It is known that the indirect $(X_1^c - \Gamma_{15}^v)$ energy gap decreases with increasing pressure in the diamond and zinc-blende-type semiconductors.[20] We believe that the same is true for the $X_1^c - \Gamma_{15}^v$ with 3C-SiC. Then it follows that 3C-SiC becomes more absorbing as pressure is increased. The situation is just opposite to the case of Ge, in which the second-order Raman scattering could be measured only at very high pressures.

We did not observe in the spectra displayed in Fig. 6 any evidence of Raman signals for Stokes shifts smaller than 700 cm^{-1}. For shifts larger than 1900 cm^{-1}, the spectra were dominated by the second-order Raman peaks from the diamond anvil.[18]

Figures 7 and 8 display the measured peak positions of the features $a-g$ of Fig. 6 as a function of the lattice compression (lower linear scale) and pressure (upper scale). The relationship between lattice constant and pressure was taken from Eq. (1) with $B_0 = 321.9$ GPa and $B_0' = 3.43$. Both

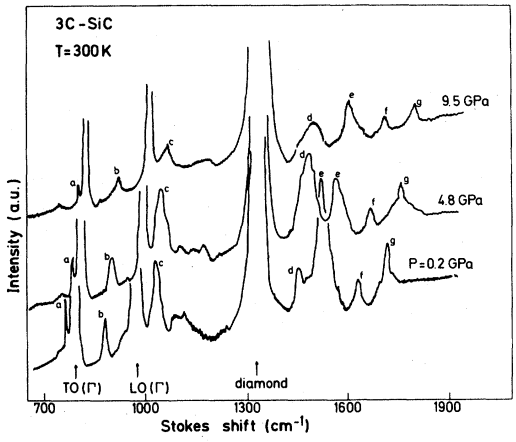

FIG. 6. Typical Stokes-Raman spectra of 3C-SiC in the 700–1900 cm^{-1} region for different values of the pressure. In this work the pressure dependence of the lines labeled $a-g$ is presented. With increasing pressure these lines shift to higher wave numbers. The combination of phonons responsible for these lines are shown in Table III. The two strong lines marked with arrows and characterized as TO(Γ) and LO(Γ) correspond to the first-order Raman lines of 3C-SiC. Their behavior on pressure has been studied separately (Ref. 8). The strongest line, which peaks at around 1330 cm^{-1} and does not shift with pressure, arises from the first-order Raman scattering of the diamond anvil.

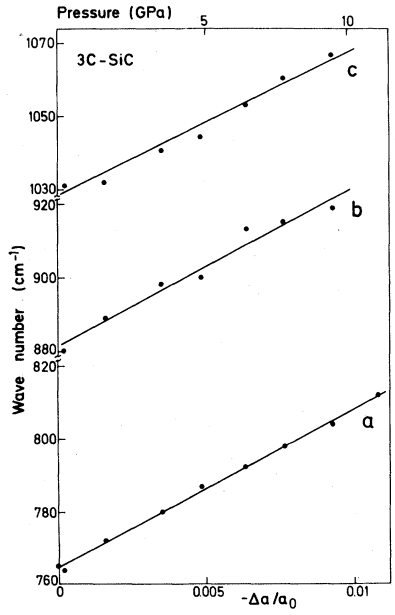

FIG. 7. Dependence on relative lattice compression (lower scale) and pressure (upper scale) of the lines *a*, *b*, and *c* of Fig. 6. The solid lines are least-squares fits with the parameters listed in Table II. For the characterization of these lines see Table III and the text.

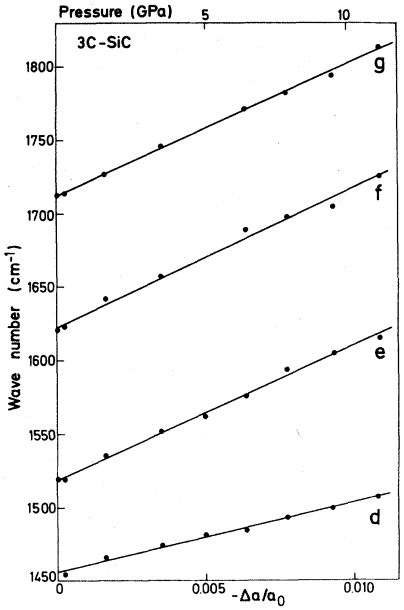

FIG. 8. Dependence on relative lattice compression (lower scale) and pressure (upper scale) of the lines *d*, *e*, *f*, and *g* of Fig. 6. The solid lines are least-squares fits with the parameters listed in Table II. For the characterization of these lines see Table III and the text.

values correspond to the average of these quantities for Si and diamond (the validity of this assumption is discussed in Ref. 8). The solid lines are least-square fits with the parameters listed in Table II. For comparison the corresponding parameters of the TO(Γ) and LO(Γ) phonons are also tabulated.[8] The coefficients A of Table II fall into two categories: for the features $a-d$ of Fig. 6 they are comparable with those of the TO(Γ) and LO(Γ) phonons. The A's of features $e-g$ are almost twice those of the optical phonons at the Γ point. It is clear that these second-order Raman lines $e-g$ arise from scattering by overtones of optical modes.

To our knowledge no measurements of the phonon dispersion curves of 3*C*-SiC with neutron scattering are available, as it is not possible to grow crystals sufficiently large for these experiments. However, experimental information for the phonon dispersion along the [111] direction has been inferred for 3*C*-SiC by measuring the first-order Raman scattering from different polytypes and using the concepts of the large zone scheme.[14] The energy of some phonons with wave vectors near the X point of the Brillouin zone have been determined from the energies of phonon replica luminescence lines for optical transitions near the $(X_1^c-\Gamma_{15}^v)$ indirect edge.[21] Theoretical calculations of the phonon dispersion curves of 3*C*-SiC have been performed.[22,23] As these calculations overestimate the energy of the acoustical branches for wave vectors in the [100] direction, we use the experimental data of Refs. 14 and 21 to interpret the Raman lines $a-g$ of Fig. 6. Table III reproduces the measured energies of the phonons at L and X and a comparison between the low-pressure results for the lines $a-g$ from Table II and the possible overtones combinations from which these lines may arise. The assignment may not be unique, particularly if one considers that the measured energies of the phonons at X correspond to low-temperature data and some shifts of these modes to

TABLE II. Dependence on relative lattice compression of the Raman lines labeled $a-g$ in Fig. 6. The data of the LO(Γ) and TO(Γ) first-order Raman lines from Ref. 8 of 3*C*-SiC are also included for comparison.

Denomination in Fig. 1	$\omega=\omega_0-A\frac{\Delta a}{a_0}$ ω_0 (cm^{-1})	$A=\frac{d\omega}{d\frac{\Delta a}{a_0}}$
a	764.8±1	4345±40
b	881.3±1	4350±40
c	1028.5±2	3994±40
d	1456.3±2	4750±40
e	1519.3±2	9100±50
f	1623.7±2	9395±50
g	1712.8±2	9144±50
TO(Γ)	796.5±0.3	3734±30
LO(Γ)	973.0±0.3	4532±30

TABLE III. Energies of several phonon modes of 3C-SiC at the zone edges and possible overtone combinations from which the Raman lines of Fig. 6 may arise.

Phonon mode[a]	Energy[a] (cm^{-1})	Overtone combination	Raman lines of Fig. 6 for $\Delta a = 0$[b]
TA(L)	266		
LA(L)	610		
TO(L)	766		
LO(L)	838		
TA(X)	373	TO(L)+TA(L)=1032	$c = 1028.5 \pm 2$
LA(X)	640	LO(L)+LA(L)=1448	$d = 1456.3 \pm 2$
TO(X)	761	2TO(X)=1522	$e = 1519.3 \pm 2$
LO(X)	829	TO(L)+LO(L)=1604	$f = 1623.7 \pm 2$

[a]From Refs. 14, 21, and 24.

[b]See discussions for the characterization of lines a, b, and g of Fig. 6.

lower frequencies are expected. However, as the pressure dependence of a phonon branch near the zone edges does not depend very strongly on the wave vector direction, we believe that no major errors are made if we choose a phonon combination at L when perhaps it could also be at X. We have done the characterization of Table III by requiring the compatibility of the low-pressure data together with the measured pressure dependence of the lines. For example, we cannot expect for the acoustical branches very large *positive* Grüneisen parameters just keeping in mind the pressure dependence of those modes in Si (Ref. 2) and diamond.[3]

The characterizations of the lines labeled with c, d, e, and f is straightforward in the way discussed above. The lines labeled a, b, and g require some more care. The low-pressure energy position of the line a can neither be fitted with an overtone combination of acoustical phonons at the X nor at the L point. On the other hand, the pressure coefficient of this line (Table II) is comparable with those at the optical phonons. In the 6H-SiC polytypes (wurtzite structure) a very strong first-order Raman line of symmetry E_2 is observed at 766 cm^{-1}.[24] This line corresponds in the large zone scheme to the zone-edge TO phonon at L.[14] The origin of the line a in Fig. 6 can be explained by assuming the presence of some random stacking (stacking faults) in the cubic sample. The line a, which peaks at 764.8 ± 1 cm^{-1} at low pressures, corresponds to a first-order Raman scattering from the layers in which the normal "*ABC ABC*" stacking of the fcc structure has changed to the "*AB AB*" stacking of the hexagonal structure. This interpretation agrees also with the fact that the dependence of this line on lattice compression is almost the same as that of the optical phonons at Γ (see Table II).

The line b peaks at 881.3 ± 1 cm^{-1} at low pressures. This energy is very close to the combination TA(L)+LA(L) from the values of Table III. However, if we adopt this phonon combination for line b it would be very hard to justify the positive A coefficient of these acoustical modes. With this characterization of line b together with the adopted phonon combination of the line c, one would obtain a large positive Grüneisen parameter for the TA(L) modes, which does not fit in the systematic behavior of other semiconductors.[2-4] As in the case of line a, line b may arise from first-order Raman scattering by atomic layers with random stacking. The energies of the A_1 axial optic modes of 6H-SiC is 889 cm^{-1},[24] which lies very close to the measured energy of the peak b. The A_1 axial optic modes of 6H-SiC correspond in the large zone scheme to LO phonons with wave vectors at around 0.7 in the Λ direction.[14,24] The characterization of line b as Raman scattering by optical modes, which become active due to stacking faults, is also in agreement with the fact that the coefficient A compares with that of the LO(Γ) phonons (see Table II).

Finally, the line at 1712.82 cm^{-1} (labeled g) cannot be fitted with a combination of optical phonons at the X or L points. The energy of this line lies between 2LO(Γ) and 2LO(X) or 2LO(L). We conjecture that this line arises from an overtone combination of optical phonons with wave vectors near the point W at the zone edges. The disper-

TABLE IV. Mode-Grüneisen parameters for a number of phonon modes of 3*C*-SiC, Si, and diamond.

Mode	3*C*-SiC[a]	Si[b]	Diamond[c]
TO(Γ)	1.56±0.01	0.98±0.06	1.19±0.09
LO(Γ)	1.55±0.01	0.98±0.06	1.19±0.09
TO(*X*)	2.0 ±0.2	1.5 ±0.1	2.0 ±0.4
TO(*L*)	1.9 ±0.20	1.3 ±0.1	1.4 ±0.25
LO(*L*)	2.0 ±0.2		1.27±0.09
TA(*L*)	−0.43±0.08	−1.3 ±0.3	
LA(*L*)	−0.17±0.04		

[a]This work.
[b]Reference 2.
[c]Reference 3.

sion curves of the optical phonons for wave vectors between the points *K* and *X* are very flat, and consequently the density of states for two phonon processes is expected to be large.[17] The corresponding energies of these optical branches lie between the LO energies at Γ and *X* or *L*, respectively. Raman scattering by overtones of phonons with wave vectors in between *X* and *K* were very often observed in the second-order Raman spectra of diamond and zinc-blende-type materials.[4,17]

With the coefficient *A* of Table II, the characterizations in Table III, and assuming that the pressure dependence of the line *a* corresponds to that of the TO(*L*) phonons, a number of Grüneisen parameters can be determined for various phonon modes of 3*C*-SiC. They are tabulated in Table IV together with similar data for Si and diamond. The trend that the Grüneisen parameters of the optical modes at the zone boundaries are larger than at the zone center is also reproduced in 3*C*-SiC. The absolute values of the Grüneisen parameters of the acoustic modes are smaller than those of other semiconductors.[4] However, the only data existing for the acoustic modes of diamond give a value of $\gamma_{TA(X)}=0.4\pm0.9$, which also does not fit in the systematic of the covalent-type materials.[3]

Having discussed the behavior under compression of the observed second-order Raman lines of 3*C*-SiC and shown that a softening of the acoustic modes takes place, we want to present the pressure dependence of the linewidth of the TO(Γ) and LO(Γ) phonons. While studying the dependence on pressure of the long-wavelength optical phonons in Ref. 8, this point was not discussed because the major interest was the behavior of the LO(Γ)−TO(Γ) splitting under pressure and of the Born's transverse effective charge. The pressure dependences of the widths of the first-order Raman lines are shown in Fig. 9. For pressures above 10.6 GPa a large increase of the linewidths is measured. This behavior was observed for all the runs performed and upon cycling the pressure. The increase of the linewidth with pressure can be qualitatively attributed to discrete-continuum anharmonic interaction. The one-phonon TO(Γ) or

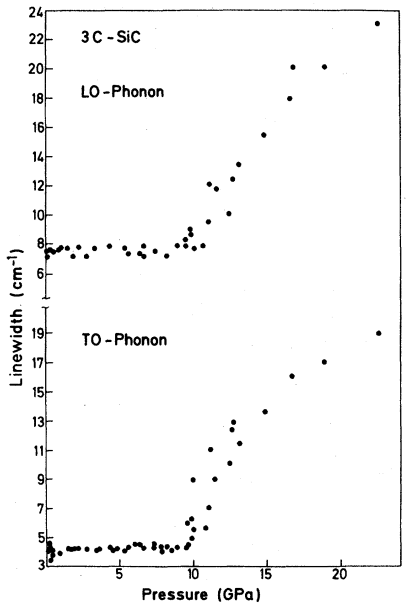

FIG. 9. Pressure dependence of the LO(Γ) and TO(Γ) Raman linewidths. For pressures above 10 GPa an increase of the width with pressure takes place, due to an increase of the decay rate of the long-wavelength optical phonons into two acoustical ones.

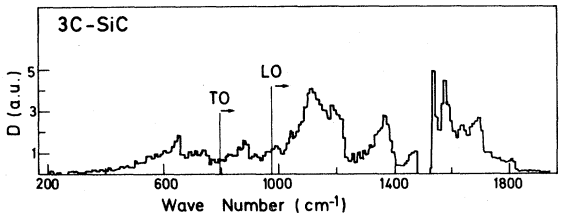

FIG. 10. Two-phonon density of states for 3C-SiC taken from Ref. 22(b). The low-pressure energy positions of the TO(Γ) and LO(Γ) phonons are also displayed. With increasing pressure these discrete lines shift to regions of higher density of states.

LO(Γ) modes decay into a continuum of two acoustical phonon modes.[25] Figure 10 reproduces the calculated two-phonon densities of states for 3C-SiC taken from Ref. 22(b). From which phonon combinations the structures of the two-phonons density of states arise was not resolved in Ref. 22(b). The low-pressure energy positions of the TO(Γ) and LO(Γ) phonons are represented by the narrow solid lines in Fig. 10. One can assume that the major contribution to the local maxima in the density of states just above the TO(Γ) and LO(Γ) energies comes from overtones of acoustical modes. With increasing pressure the one-phonon lines shift to higher energies while the continuum of acoustical modes shifts to lower energies. The discrete lines enter into a region of larger density of states, a fact which produces an increase in the decay rate of the long-wavelength optical modes into acoustical ones. Hence an increase of the Raman linewidth is measured as a consequency of the decrease of the optical phonon lifetime. Coupling (increase of the phonon linewidth) or decoupling (decrease of it) of a discrete phonon line with a continuum of two phonons due to the influence of the pressure have also been reported previously for GaS (Ref. 26) and GaP (Ref. 2).

ACKNOWLEDGMENTS

We want to thank Dr. W. J. Choyke for the samples of 3C-SiC. The help of Mr. W. Dieterich in loading the diamond cell is gratefully appreciated.

[1]J. D. Barnett, S. Block, and G. J. Piermarini, Rev. Sci. Instrum. 44, 1 (1973); G. J. Piermarini, S. Block, J. D. Barnett, and R. A. Forman, J. Appl. Phys. 46, 2774 (1975).
[2]B. A. Weinstein and G. J. Piermarini, Phys. Rev. B 12, 1172 (1975).
[3]B. J. Parson, Proc. R. Soc. London Ser. A 352, 397 (1977).
[4]R. Trommer, H. Müller, M. Cardona, and P. Vogl, Phys. Rev. B 21, 4869 (1980).
[5]R. Trommer, E. Anastassakis, and M. Cardona, in *Light Scattering in Solids,* edited by M. Balkanski, R. C. C. Leite, and S. P. S. Porto (Flammarion, Paris, 1976), p. 396; R. Trommer, Ph.D. thesis, University of Stuttgart, 1977 (unpublished).
[6]B. A. Weinstein, Solid State Commun. 24, 595 (1977).
[7]C. Carlone, D. Olego, A. Jayaraman, and M. Cardona, Phys. Rev. B 22, 3877 (1980).
[8]D. Olego, M. Cardona, and P. Vogl, Phys. Rev. B (in press).
[9]H. Wendel and R. M. Martin, Phys. Rev. B 19, 5251 (1979).
[10]T. Soma, Y. Saitoh, and H. Matsuo, Solid State Commun. 39, 913 (1981).
[11]C. J. Buchenauer, F. Cerdeira, and M. Cardona, in *Light Scattering in Solids,* edited by M. Balkanski (Flammarion, Paris, 1971), p. 280.
[12]F. Cerdeira, C. J. Buchenauer, F. H. Pollak, and M. Cardona, Phys. Rev. B 5, 580 (1972).
[13]B. Welber, M. Cardona, Y. Tsay, and B. Bendow, Phys. Rev. B 15, 875 (1977).
[14]D. W. Feldman, J. Parker, W. Choyke, and L. Patrick, Phys. Rev. 173, 787 (1968).
[15]K. Syassen and W. Holzapfel, Phys. Rev. B 18, 5826 (1978).
[16]H. J. McSkimin, A. Jayaraman, and P. Andreatch, J. Appl. Phys. 38, 2362 (1967).
[17]B. A. Weinstein and M. Cardona, Phys. Rev. B 7, 2545 (1973).
[18]S. A. Solin and A. K. Ramdas, Phys. Rev. B 1, 1687 (1970).
[19]R. G. Humphreys, D. Bimberg, and W. J. Choyke, Solid State Commun. 39, 163 (1981).
[20]D. Olego, M. Cardona, and H. Müller, Phys. Rev. B 22, 894 (1980).
[21]W. J. Choyke, D. R. Hamilton, and L. Patrick, Phys. Rev. 133, A1163 (1964).
[22](a) K. Kunc, M. Balkanski, and M. A. Nusimovici, Phys. Status Solidi B 72, 229 (1975); (b) K. Kunc, Ph.D. thesis, University of Paris VI, 1975 (unpublished).
[23]T. N. Singh, S. S. Kushwaha, and G. Singh, Solid

State Commun. 13, 1393 (1973).
[24]D. W. Feldman, J. Parker, W. Choyke, and L. Patrick, Phys. Rev. 170, 698 (1968).
[25]D. Olego and M. Cardona, Phys. Rev. B (in press).
[26]A. Polian, J. M. Beson, J. C. Chervin, and A. Chevy, in *High Pressure Science and Technology,* edited by B. Vodar and Ph. Marteau (Pergamon, New York, 1980), p. 517.